Journal of Innovations in Business and Industry

aspur

Vol. 03, No. 02 (2025) 145-152, doi: 10.61552/JIBI.2025.02.008 - http://jibi.aspur.rs

AERODYNAMIC MODELING OF ROCKETS WITH RASAERO II

Amr Abbass [1]

Received 28.02.2024.
Revised 01.05.2024.
Accepted 24.05.2024.

Keywords:
Rasero II, rocket, aerodynamic, modeling.

Original research

A B S T R A C T

This research investigates the use of RASAero II, an advanced aerodynamic analysis and flight simulation software, in the design and evaluation of rocket vehicles. In addition to highlighting the software's powerful input system, it also discusses the many techniques used to reproduce accurate flight conditions. RASAero II allows users to customize nose cones, fuselage tubes, fins, and protuberances, among other features. These modifications affect the stability and aerodynamics of the rocket. By integrating complex inputs. The properties of the fin profile, and the rail guide measurements, the software enables accurate modeling of the aerodynamic forces and moments. Stability assessments can also be made more accurate by using Rogers' modified Barrowman method and providing alternatives for turbulent flow analysis. The study also emphasizes how pitch and yaw rotations dynamically affect the rocket.

1. INTRODUCTION

This study explores the intricate aerodynamic characteristics of rockets as they move through the atmosphere, with a specific emphasis on the pressure distributions and forces that arise as a result. Through the analysis of both equilibrium and nonequilibrium states, this study emphasizes the impact of compressibility, ablation, and radiation on high-speed flows (Wang et al., 2023). The study highlights the importance of accurate aerodynamic modeling and the use of Computational Fluid Dynamics (CFD) to enhance rocket design and performance.

2. LITERATURE REVIEW

Aerospace engineering's rocket aerodynamics is a significant topic, and RASAero II and other modeling tools are essential for optimizing designs and guaranteeing flight stability. The application, improvement, and validation of RASAero II have been the subject of several studies, which have deepened our understanding of rocket aerodynamics.

In Milne et al. (2023), Rose and Niemeyer (2021) demonstrate how the program can model intricate aerodynamic events, giving rocket designers sophisticated forecasting capabilities. The accuracy of RASAero II's modeling of aerodynamic coefficients and flow dynamics—which is necessary for precise flight predictions—is highlighted in this work.

The Cadamuro et al. (2024) and Schoch (2023) compares different prediction techniques with RASAero II. According to his research, RASAero II predicts stability parameters more accurately than conventional techniques, particularly in supersonic and transonic flight regimes.

The impact of various fin shapes on rocket performance is examined in Sankalp et al. (2022), Schoch (2023) and Barokah et al. (2024). Slabber et al. (2024) shows how optimized fin designs greatly increase stability and decrease aerodynamic drag, boosting overall flying efficiency using RASAero II.

In Rose and Niemeyer (2021), Chaowanapreecha and Rattanagraikanakorn (2023) close the gap between simulation and real-world application. This research emphasizes the significance of combining simulation results with experimental findings to obtain optimal

[1] Corresponding author: Amr Abbass
Email calgary732@outlook.com

rocket designs by validating RASAero II's predictions using experimental data and demonstrating its reliability in real-world circumstances.

In Hannaford et al, (2020) explains how to compute important aerodynamic coefficients using the program. The precision and effectiveness of RASAero II's computational approaches for aerodynamic analysis are highlighted in this publication, which also discusses them.

Huh and Kwon (2022) explore the difficulties associated with simulating multi-stage rockets. Hannaford et al, (2020) case study demonstrates how RASAero II can accurately simulate each stage's aerodynamic behavior, guaranteeing thorough analysis and improved design optimization.

Harahap et al. (2020) discusse the advantages of merging aerodynamic simulations with structural analysis. This study demonstrates that by taking into account both aerodynamic forces and structural integrity, RASAero II's integration capabilities enable more reliable and accurate flight predictions. Stoldt et al. (2021) discusses the intricacies of turbulent flow conditions. He outlines the approaches used by RASAero II to forecast stability in these kinds of circumstances, showcasing the flexibility and accuracy of the program.

In Rose (2021). assesses the method's accuracy within RASAero II. According to his research, using this technique in RASAero II improves the precision of high-speed flight forecasts. The impact of surface roughness on aerodynamic performance is examined in Jung, and Baeder (2020). Jung and Baeder (2020) provides important insights into how surface texture impacts drag and stability by simulating various roughness conditions using RASAero II. Żurawka et al. (2023) delves into the fundamentals of boosted dart rocket design using RASAero II. Green emphasizes how the program can improve design parameters and simulate distinct aerodynamic profiles for these niche rockets.

Muslimin et al. (2023) focused on using the program in educational environments. Lewis shows how RASAero II, which gives students practical experience in rocket design and aerodynamics, may be a useful teaching tool.

Sorrel et al. (2024) looks at integrating real-time atmospheric data into simulations, according to thisresearch, using this data greatly increases the precision of flight forecasts, increasing the adaptability and dependability of RASAero II.

Lippmann et al. (2021) explores possible software developments. Evans indicates that RASAero II has a bright future by outlining areas for improvement, such as improved computing techniques and better interface with other simulation tools.

Together, these investigations highlight how reliable and flexible RASAero II is for simulating rocket aerodynamics. RASAero II is a valuable tool for rocket design and research, offering advanced simulation methodologies, comparative studies, practical applications, and educational value. As a premier software in aeronautical engineering, it will be further solidified by future developments and ongoing validation through experimental data.

3. GENERAL OVREVIEW

The local airflow surrounding a rocket's body is forced to alter its speed as it travels through the atmosphere. A complicated pressure field is created across the vehicle's skin or surface as a result of these speed variations. Air is deemed incompressible at low subsonic speeds, which means that as it passes around the vehicle, its density does not vary much. The primary cause of the pressure variations is variations in air flow velocity. According to Bernoulli's principle, a decrease in pressure and an increase in fluid velocity happen at the same time. Air becomes compressible and density variations start to matter at speeds greater than roughly Mach 0.7. Shock waves and other phenomena brought on by compressibility factors alter the rocket's pressure distribution. At zero angle of attack, the airflow around the rocket nose and fuselage is symmetrical. At the very tip of the nose, the airflow velocity is zero, creating a stagnation point where the pressure reaches its highest. As one advances away from the stagnation point along the surface of the nose, pressure decreases as airflow accelerates around the curvature of the nose. The lines illustrating this pressure distribution show areas of suction (lower pressure) except at the stagnation point. An axisymmetric pressure distribution is the result of the flow being symmetrical about the rocket's longitudinal axis. The pressure distribution's symmetry is broken as the angle of attack increases. The increased flow velocity across these regions causes an increase in pressure on the rocket's lower surfaces. The rocket experiences a lifting force as a result of this higher pressure. Conversely, when the flow speeds across these regions, the pressure on the upper surfaces drops, resulting in suction. More lift and pitching moments are produced by this pressure differential between the top and bottom of the object. It is possible to convert the pressure distribution into various reference axes to facilitate an easier examination of the aerodynamic forces.

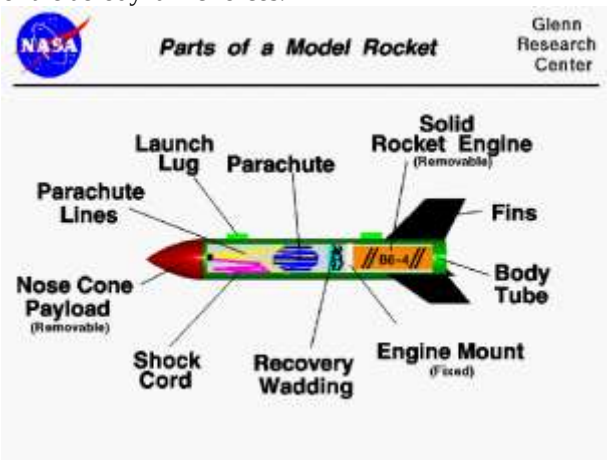

Figure 1. Parts of Model Rocket (Nasa Web site)

The forward fuselage portion and the nose are part of the front fuselage (Figure 1, Figure 2). Changes in the direction and speed of air flow cause notable variations in pressure in this region. For stability and control, the rocket's fins in the tail are essential.

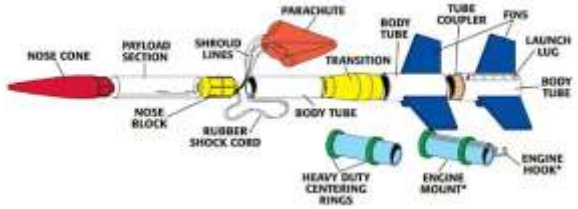

Figure 2. Parts of Rocket

You feel pressure distributions that produce aerodynamic forces and moments that stabilize. Drag and lift coefficients could be used to describe the flow around the rocket.

4. METHODOLOGY

Pressure Distribution and Forces

Aerodynamic forces, which act at the centroid of the pressure distribution, or "centers of pressure," can then be obtained by integrating the pressure distribution across the whole skin surface. In the early days of aerodynamics, it was discovered that the combined aerodynamic forces and the pressure values in the pressure distribution were a function of:

$$F = qSC$$

$$\text{force} = \frac{1}{2}\rho V^2 S C_f$$

Axes Systems in Rocket Aerodynamics

It is essential to comprehend the axis systems utilized to characterize aerodynamic forces on rockets in order to analyze their performance and behavior. The two most widely utilized aerodynamic force axis systems are body axes and wind axes. The aerodynamic forces in the Wind axes system are related to the direction of freestream flow, which is also referred to as the incoming "wind." In aerodynamics, this method is more frequently utilized in aircraft. The forces are resolved into the Wind axes system. The geometric axes of the vehicle, such as the axes of symmetry, are referred by the forces in the body axis system. In rocketry, this approach is more frequently utilized.

The Barrowman analysis

NASA aerodynamicist and rocketeer James Barrowman chose to try and determine the lift coefficient (Normal coefficient), and centers of pressure, of the forebody and fins (and boattail) of a rocket vehicle at near-zero angle of attack.

He created some pretty basic equations by mathematically replicating the flow around the vehicle and ignoring the effects of viscosity and freestream Mach number. As we'll see, however, his calculations provide results that are quite accurate when compared to the more intricate equations we'll employ later. He found that, for all standard nose cone designs, the lift curve slope for the nose at zero angle of attack equals 2.0 and that, at nearly zero angle of attack, the lift of the fuselage was zero. ,R=2.0 (per radian) for,B-O.

He computed the fins lift curve slope in two halves at zero alpha. first, the fins' alone lift:

$$C_{N\propto 0 \text{ fin}} = \frac{4n\left(\frac{s}{d}\right)^2}{1+\sqrt{\left(1+\left(\frac{2L_F}{C_R+C_T}\right)^2\right.}} \text{ (per radian)}$$

The airflow across the fuselage in front of the fins was then added by him.

Interference factor $= 1 + \frac{r}{s+r}$

In these equations:

$n =$ number of fins (3 or 4)

$d =$ fuselage diameter

$r =$ fuselage radius

$s =$ fin semi-span (NOT area)

$L_F =$ length of midchord

$C_R =$ root chord length

$C_T =$ tip chord length

He discovered that the lift of a boat-tail with a straight cone is negative, meaning it faces the opposite direction of the lift from the fin and nose. Its lift he derived as:

$$C_{\text{Nocoboat}} = -2\left(1-\left(\frac{d_R}{d}\right)^2\right) \text{ (per radian)}$$

which is negative. The boat-tail's reduced diameter is represented by d.

The following formula can be used to find any aerodynamic surface's center of pressure (X) at zero angle of attack:

$$\frac{X}{d} = -\frac{C_{m\alpha 0}}{C_{N\alpha 0}}$$

Where measured about the nose-tip, is the gradient of the pitching moment coefficient curve (per radian) at zero angle of attack. The position of the center of pressure, measured aft of the nose-tip, is thus obtained. Keep in mind that the center of pressure location is given in calibers by this formula. To convert to meters, multiply by the fuselage diameter, or "d".This formula was used by Barrowman to determine the center of pressure of a tangent-ogive nosecone, which is the shape that most of our nosecones have.

$$X_{\text{nose}} = 0.466 L_N$$

where measured from the tip of the nose after, Lc is the nosecone's length (in meters). Thus,,-nose. in meters is obtained. He deduced the following for the fins' center of pressure (meters aft of nose tip):

$$X_{Fins} = X_B + \frac{X_R}{3}\left(\frac{C_R + 2C_T}{C_R + C_T}\right) + \frac{1}{6}\left(C_R + C_T - \frac{C_R C_T}{C_R + C_T}\right)$$

Where ,-R. and ,X-B. are lengths . For the straight-cone boat-tail center of pressure (meters aft of nose tip) he derived:

$$X_{\text{boat}} = X_P + \frac{L_T}{3}\left(1 + \frac{1 - \frac{d}{d_R}}{1 - \left(\frac{d}{d_R}\right)^2}\right)$$

Barrowman's Analysis of Rocket Stability

The work of James Barrowman offers a fundamental method for assessing the static stability of fixed-fin rocket launchers, especially in the vicinity of liftoff. His approach, which is frequently summed up as Barrowman's equations, is essential for guaranteeing that rockets fly with their noses forward, which is necessary for aerodynamic stability and efficient trajectory control.

Static Stability Analysis

In rocketry, static stability refers to a rocket's innate inclination to keep or revert to its original flight path in the event of a disturbance, like a wind gust. Static stability analysis, in contrast to dynamic stability, does not take into account the vehicle's rotational dynamics with respect to its center of gravity (CG).Fundamental Ideas in Barrowman's Stability Analysis Gravity Center (CG).All rotational movements naturally revolve around this point. Additionally, it is the location where the total moment caused by gravity forces equals zero. Center of Pressure (CP).This is the location on the rocket's body where the total aerodynamic pressure forces, which are caused by airflow contact and are dispersed over the surface, can be said to be at work. The moments (torque effects) produced by the aerodynamic forces at the fins and forebody are compared as part of the stability study. The space between these components' CG and CP is known as the moment arm. When the moment created by the fins about the CG is larger than the moment created by the forebody, the stability requirement is satisfied.

Moment Arms and Forces:

The moments (torque effects) produced by the aerodynamic forces at the fins and forebody—which includes the nosecone and, if present, the boat tail—are compared as part of the stability study. The space between these components' CG and CP is known as the moment arm. When the moment created by the fins about the CG is larger than the moment created by the forebody, the stability condition is satisfied:

$$l_1 N_{\text{fins}} > l_2 N_{\text{forebody}}$$

where the distances from the CG to the forebody and fins, respectively, are denoted by,l-2 and,l-1.The Restoring Moment Equation.

The stabilizing restoring moment M about the CG is found by using the formula: M=,-1.,N-fins.−,l-2.,N-forebody.

The moment coefficient, C-M, can be obtained from this for dimensionless analysis:

$$C_M = \frac{M}{qSd} = \frac{l_1 C_{N_{\text{fins}}} - l_2 C_{N_{\text{facebody}}}}{d}$$

Here, d is the dynamic pressure, l is the reference area, and l is the reference length (usually the fuselage diameter). Compute the Total Center of Pressure By calculating the weighted average of the centers of pressure for each aerodynamic component—the fins, the forebody, and any additional pieces like boat tails—Barrowman's equations enable the computation of the total center of pressure:

$$X_{\text{CP overall}} = \frac{C_{N_{\text{farebody}}} X_{\text{forebody}} + C_{N_{\text{fins}}} X_{\text{fins}} + C_{N_{\text{boat-toll}}} X_{\text{boat-tail}}}{C_{N_{\text{forehody}}} + C_{N_{\text{fins}}} + C_{N_{\text{boat-tall}}}}$$

Static Stability Margin:

A crucial metric known as the Static Stability Margin quantifies the amount (measured in fuselage diameters, or calibers) that the total CP lags behind the CG. About 1.5 calibers is a normal amount for sufficient stability, though this can change depending on the wind, speed, and shape of the vehicle during flight.

Dynamic Effects in Rocket Aerodynamics

Rocket dynamic stability takes into account the impacts of rotation and angular motions, which affect the aerodynamic forces that different parts of the vehicle—like the nose, fins, and boat-tail—experience. The local angle of attack along the vehicle's body is changed by these rotations, which has an impact on the aerodynamic loading and, in turn, the stability of the vehicle.

Understanding Dynamic Aerodynamic Effects

A rocket's pitching up causes dynamic changes in the angle of attack, which alter the rotation and velocity vectors throughout the rocket's structure. The rocket's center of gravity (CG) rotates pitch-up, changing the relative wind angle in various parts of the vehicle. Because of their various distances from the center of gravity, the fins, forebody, and boat-tail suffer varied effective wind angles.

Compute the Dynamic Angle of Attack. Both the static angle of attack (derived from the vehicle's trajectory) and the dynamic contributions from rotational motion affect the angle of attack for each component (forebody, fins, and boat tail):

$$\alpha_{\text{dynamic}} = \alpha_{\text{static}} \pm \frac{l\dot{\theta}}{V}$$

Here, the airspeed is V, the pitch rate is θ, the distance from the component's center of pressure to the center of pressure is l, and the angle of attack caused by the vehicle's motion is α-static. Damping by Aerodynamics A vital component of rocket stability, aerodynamic damping aids in keeping the vehicle stable against rotational disturbances:

Impact on Lifting Forces By changing the local angles of attack, rotation increases lift on the tail and fins and decreases it on the nose. By tending to offset the rotation, this distribution produces aerodynamic damping, a stabilizing effect.

The representation of mathematics: Calculations are made simpler by assuming modest angle approximations, $\cos(\alpha)\approx 1$ and $\sin(\alpha)\approx\tan(\alpha)\approx\alpha$ (in radians). The following formula is used to calculate each component's dynamic angles of attack:

$$\alpha_{\text{component}} = \tan^{-1}\left(\frac{V_v}{V_u}\right) \pm \frac{l\dot{\theta}}{V}$$

The normal and axial components of the airflow velocity stability analysis and lift coefficients are denoted by, Vv. and, Vu.The total of all aerodynamic components' contributions is used to compute the overall normal (lift) force and the ensuing pitching moment:

$$N = \frac{1}{2}\rho V^2 S\left(C_{N_{\text{foreblody}}} + C_{N_{\text{fins}}} + C_{N_{\text{bout-tall}}}\right)$$

$$M = \frac{1}{2}\rho V^2 S\left(C_{N_{\text{foreb body}}} l_2 - C_{N_{\text{fins}}} l_1 - C_{N_{\text{boat-tall}}} l_3\right)$$

Here, S is the reference area, $\boldsymbol{U}$-N are the normal force coefficients, and l values are the separations between the respective centers of pressure and the CG.

In order to guarantee that rockets are built to withstand the intricate relationships that arise between rotational dynamics and aerodynamic forces throughout their flight envelope, dynamic stability considerations are crucial.

Simulation Using RASAero II

- There are several different nose cone forms available for the RASAeroII Nose Cone Inputs, including ogive, conical, and parabolic. The drag and stability of the rocket are impacted differently by each shape. The nose cone's diameter and length are entered by users, and the program determines the associated aerodynamic properties.
- Rail Guide/Launch Lug/Launch Shoe Inputs, Body Tube, and Fins The rocket's body tube serves as its primary structural element. Its length, diameter, and material characteristics are input.
- Fin design, size, and placement are carefully considered because they are essential for maintaining the rocket's stability during flight. In order to guarantee the rocket's correct alignment and a smooth launch, additional components are used: rail guides, launch lugs, and launch shoes. Specific inputs are needed for their dimensions and placements.
- Fin Airfoil Inputs. There are several different types of airfoil profiles, such as symmetric, cambered, and custom shapes, and these shapes have a significant impact on the aerodynamic performance of fins. The software computes lift and drag coefficients based on user-inputted parameters such as airfoil type, thickness, and other pertinent details.
- Body Tubes: Software offers the ability to install and configure extra body tubes for rockets with intricate designs that use several body tubes. The ability to describe each body tube with its own length, diameter, and material characteristics makes it possible to represent in detail multi-stage rockets or rockets with extra payload sections.
- Launch Shoe, Launch Lug, and Rail Guide Inputs Stable launch trajectory of the rocket is guaranteed by rail guides, launch lugs, and launch shoes. Users need to enter their measurements, where they are on the rocket body, and any other aerodynamic features. In order to reduce drag and guarantee a straight launch, proper positioning and dimensions are essential.
- Protuberance Data Sources The size, shape, and placement of protuberances, such as antennae, camera mounts, and other exterior fixtures, can have an impact on the rocket's aerodynamics. By simulating these protuberances, one can precisely determine how they will affect the rocket's performance during flight.
- Transitional Inputs Transitions are used to smoothly join body tubes of varying sizes. This guarantees structural integrity and correct aerodynamic modeling.
- Fin Canister Inputs Some rocket designs contain fins and add further structural support using fin canisters. Users enter the size of the canister, its material composition, and the quantity and arrangement of its fins.
- Boattail Data By tapering the back end, a boattail lowers the rocket's base drag. Users input the length, form, and beginning and ending diameters of the boattail. This data was required to compute the drag reduction and its impact on overall performance.
- The ascent of orbital launch vehicles can be simulated by running Orbital Launch Vehicle software. Users enter the desired orbit, launch parameters, and configuration of the rocket. Aerodynamic data for the ascent is generated by the program, which aids in trajectory optimization for a successful orbit insertion.
- Equivalent Surface Finish Sand Roughness Input The rocket's aerodynamic characteristics are influenced by its surface finish, which also needs to take into consideration how surface roughness influences drag and overall performance.
- Rogers had Barrowman changed. Choice of Method This technique offers a different way to figure out the rocket's aerodynamic stability. To provide more thorough design validation, users can use this option to compare results with the conventional Barrowman technique.
- Every Option for Turbulent Flow Assuming turbulent flow can lead to more accurate aerodynamic calculations for rockets operating at high speeds. Users can activate this feature on the software to mimic how turbulent flow affects the rocket's performance.
- Tests that mimic the rocket's flying characteristics are carried out. comprehensive results, such as performance measures, stability margins, and trajectory charts. Users can assess the design and make the required modifications and Aero Runs with

the aid of these results. A large motor database is used to choose the rocket motor.

Data Validation of RASAero II using different methods

RASAero II flight simulation compared with barometric altimeter data, optical tracking data, and accelerometer-based flight data.

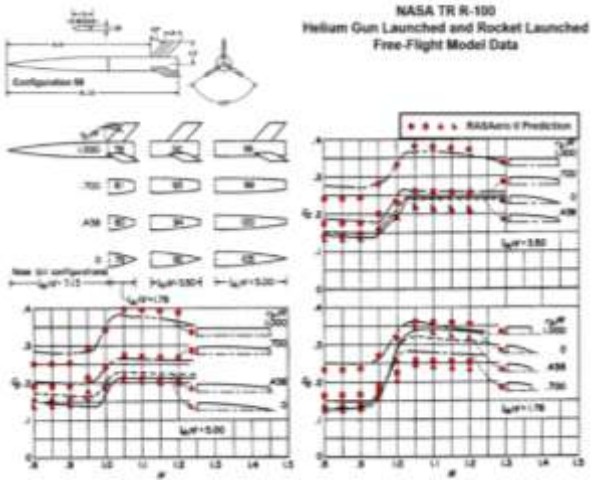

Figure 3. NASA TR R-100 Helium gun launched and rocket launched free-flight model data

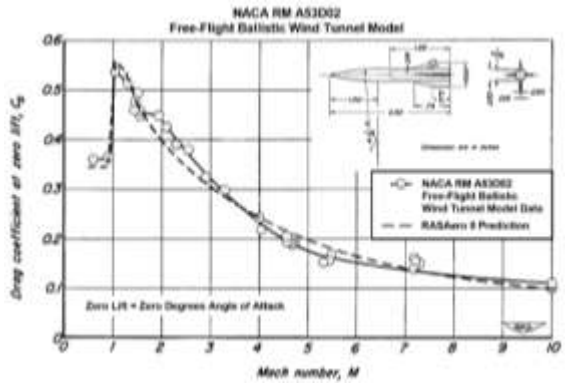

Figure 4. NACA RM A53D02 Free flight ballistic wind tunnel model

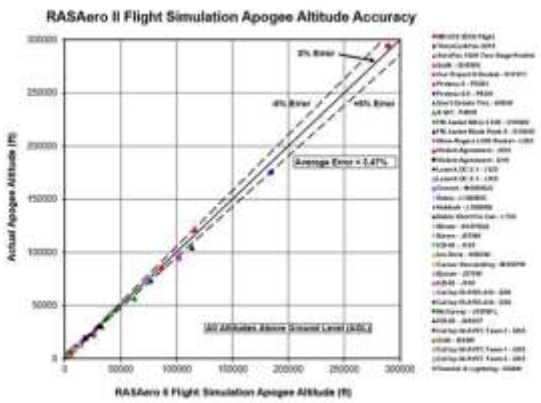

Figure 5. Apogee Altitude Accuracy "RASAERO Web site"

Data Validation of RASAero II using different methods :

- NASA TR R-100 Helium gun launched and rocket launched free-flight model data (Figure 3).
- NACA RM A53D02 Free flight ballistic wind tunnel model (Figure 4).
- Apogee Altitude Accuracy "RASAERO Web site" (Figure 5)

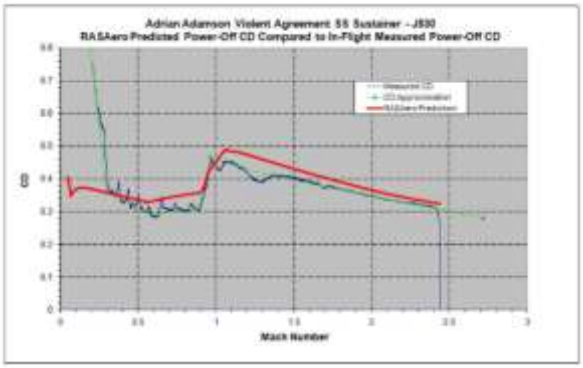

Figure 6. RASAERO Predict power off

Based on on-board accelerometer data, RASAero II estimated power-off drag coefficient (CD) during the coast phase of the Violent Agreement SS Sustainer J530 flight and compared it to in-flight measured power-off CD "RASAERO Web site" Figure 6.

Modeling Example

The Model demonstrates a Rocket with a Tangent Ogive Nose Cone and length 11.25 in, a Body Tube of Diameter 3.1 in and length 48 in with 2 BlackSky 3/8 in Railguides and 4 Fins. The liftoff Weight is 3.41 lbs and launch site elevation of 2302 MSL and 77F Deg launch angle of 3 degree . The Motor is Cesaronil I205 Nozzle Exit Data =0.63 . Case Model Rocket is presented on figure 7.

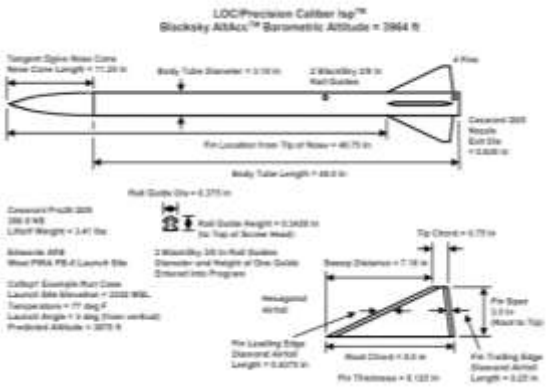

Figure 7. Case Model Rocket "RASAERO Web site"

Some results of modeling example are presented on Figure 8, Figure 9 and Figure 10.

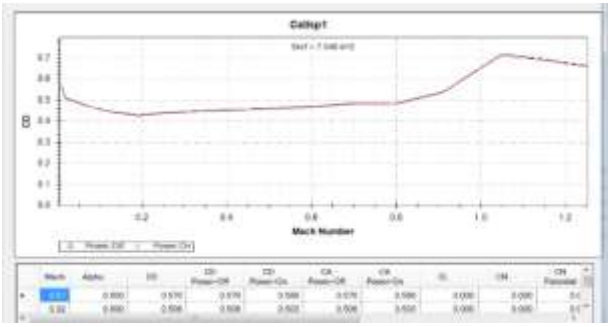

Figure 8. Aero plots for Case Rocket with CD versus Mach Number "RASAERO Web site"

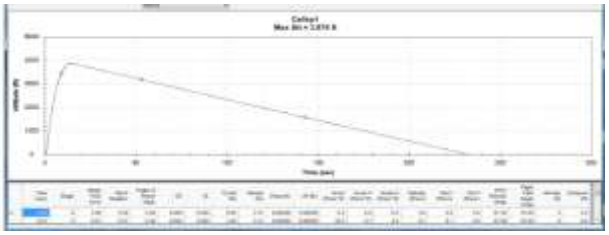

Figure 9. The Maximum Lif Versus Time , it is clear that maximum lif occurs during first 15 sec "RASAERO Web site"

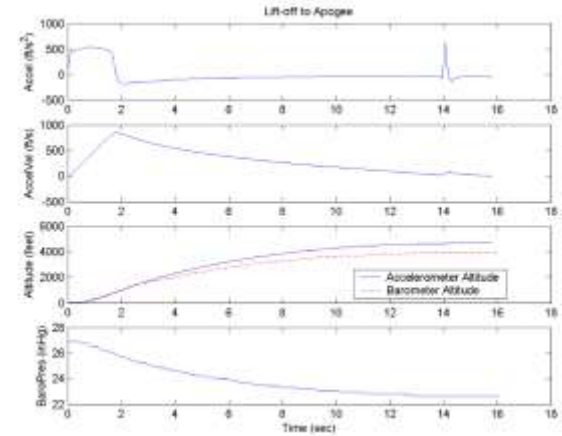

Figure 10. Barometer Altitude Accelerometer 3964 feet was the altitude determined by the on-board barometric altimeter

The actual barometric altimeter measured altitude is 3876 feet, which is only -2.22% off from the altitude predicted by the RASAero II flight simulation. "RASAERO Web site".

The Study will be extended for another two optional designs and compare it to the original design case

1. Increase the diameter of the exit Nozzle;
2. Utilizing a more powerful motor I205-300CC125J (HT).

The following are results summary and they are presented on figures 11, 12, 13, 14 and 15.

	Motor(s) Loaded	Max Alt (ft)	Max Vel (ft/sec)	Time to Apogee (sec)
▶	I205 (CTI)	3,876	723.3	14.1
	I205 (CTI)	3,965	739.7	14.2
	I205-300CC125J (HT)	4,643	824.5	14.7
*				

Figure 11. Design Extension and effect on the Maximum Altitude and Time to Apogee

Data are presented for two cases:

- Case one original case;
- Case two with increase of exit Nozzle to 1.2 inch and case three using a more powerful Motor.

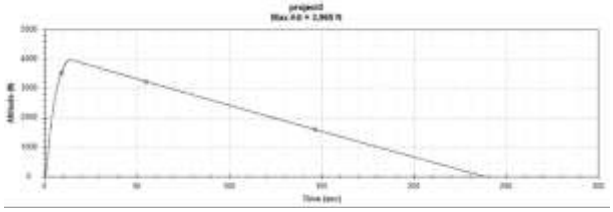

Figure 12. Increase of Nozzle Diameter and effect on Maximum Altitude

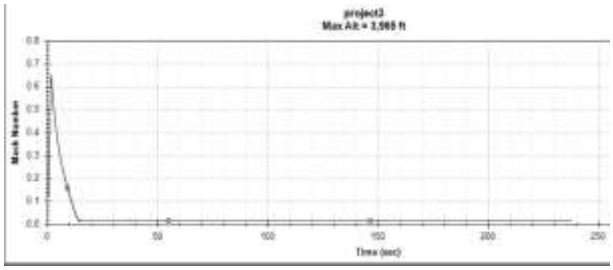

Figure 13. Increase of Nozzle Diameter and effect on Mach Number

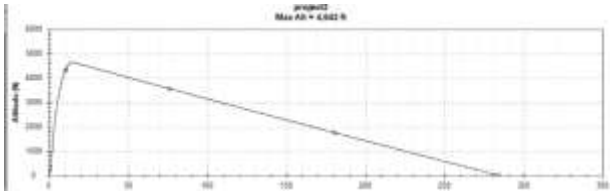

Figure 14. Change of Motor and effect on Altitude

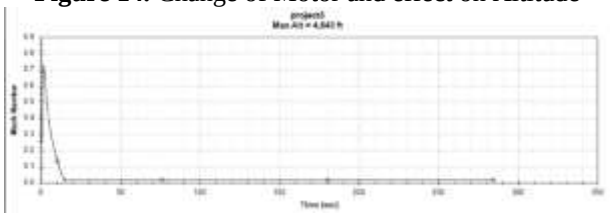

Figure 15. Change of Motor and effect on Mach Number

5. CONCLUSIONS

RASAero II represents a significant technological advance in the field of rocket simulation with its all-inclusive and user-friendly interface for aerodynamic analysis and rocket flight simulation. Because the program can handle a wide range of inputs and configurations, this article has demonstrated that it can imitate nearly any rocket design. RASAero II provides accurate aerodynamic performance, stability, and recovery dynamics predictions for a wide range of vehicles, including complex multi-stage and orbital vehicles and basic single-stage rockets. The software's integration of many aerodynamic models, including the Rogers Modified Barrowman Method and options for turbulent flow analysis, enables precise stability assessments under a variety of flight conditions. All things considered, with powerful capabilities that push the boundaries of traditional rocketry modeling and

design, RASAero II is an essential tool for aerospace engineering schools and workplaces. The software has many operating settings for the rocket's structure, motor choice, and launch circumstances. It also has some turbulent modeling, which provides a wealth of opportunities for researching alternate designs.

References:

Barokah, A. D. N., Lenggana, B. W., Wibawa, L. A. N., Turnip, A., Joelianto, E., & Le Hoa, N. (2024). A Comparative Analysis of Aerodynamic Performance: Straight Fin and Curved Fin Rockets using Computational Fluid Dynamics (CFD). *Journal of Advanced Research in Fluid Mechanics and Thermal Sciences*, *115*(1), 1-18.

Cadamuro, R., Cazzola, M. T., Lontani, N., & Riboldi, C. E. (2024). A Static Stability Analysis Method for Passively Stabilized Sounding Rockets. *Aerospace*, *11*(3), 242.

Chaowanapreecha, P., & Rattanagraikanakorn, P. (2023). Simulation-Based Design Framework for Supersonic University Sounding Rocket Project. In *2023 Regional Student Conferences* (p. 75759).

Hannaford, R., Gase, J., Reppa, M., & Lewis, H. (2020). Research and Design of a Two-Stage Supersonic Rocket.

Harahap, A. I., Bura, R. O., & Ruyat, Y. (2020, June). Modeling And Simulating The Design of Air Defense Missile Aerodynamic Systems. In *Journal of Physics: Conference Series* (Vol. 1566, No. 1, p. 012068). IOP Publishing.

Huh, J., & Kwon, S. (2022). A practical design approach for a single-stage sounding rocket to reach a target altitude. *The Aeronautical Journal*, *126*(1301), 1084-1100.

Jung, Y. S., & Baeder, J. (2020). Simulations for effect of surface roughness on wind turbine aerodynamic performance. In *Journal of physics: conference series* (Vol. 1452, No. 1, p. 012055). IOP Publishing.

Lippmann, R., Kletschke, L., Schmohl, R., Khan, E., Buchmann, B., Burnicki, A., ... & Adirim, H. (2021). Overview of the Current Work on the Student Rocket DECAN-AQUARIUS at the TU Berlin. *Dtsch Luft-und Raumfahrtkongress*, 1-10.

Milne, B., Samson, S., Carrese, R., Gardi, A., & Sabatini, R. (2023). High-Fidelity Dynamics Modelling for the Design of a High-Altitude Supersonic Sounding Rocket. *Designs*, *7*(1), 32.

Muslimin, A. N., Triharjanto, R. H., & Ruyat, Y. (2023, December). Structure design of wrap-around deployable stabilizer for 300 mm class artillery rockets. In *AIP Conference Proceedings* (Vol. 2941, No. 1). AIP Publishing.

Rose, T. J. (2021). Optimization & Qualification of a Liquid Engine Launch Vehicle Design Using 6DoF Simulations.

Rose, T. J., & Niemeyer, K. E. (2021). A Statistical Approach to Design of a Liquid Engine Launch Vehicle. In *AIAA Propulsion and Energy 2021 Forum* (p. 3355).

Sankalp, S. S., Sharma, V., Singh, A., Salian, A. S., & Srinivas, G. (2022). Computational analyses of tail fin configurations for a sounding rocket. *Aerospace Systems*, *5*(2), 233-246.

Schoch, A. (2023). Rocket stability assessment: CFD analysis of fin shapes and their impact on the static stability of a sounding rocket.

Slabber, E. R., Snedden, G., Velthuysen, T. J., Brooks, M. J., Bergh, J., & Odayan, R. (2024). Optimization of Rocket Fins using a 6-DOF Solver. In *AIAA SCITECH 2024 Forum* (p. 0380).

Sorrel, M., Herrin, C., Maybee, M., Carter, T., Fenton, K., Frank, B., ... & Frederick, R. A. (2024). 2023 University of Alabama in Huntsville Student Launch Rocket Program. In *AIAA SCITECH 2024 Forum* (p. 1340).

Stoldt, H., Quinn, D., Kavanagh, J., & Johansen, C. T. (2021). MAPLEAF: A Compact, Extensible, Open-Source, 6-Degrees-of-Freedom Rocket Flight Simulation Framework. In *AIAA Propulsion and Energy 2021 Forum* (p. 3267).

Wang, R., Wang, Z., Ma, T., Yuan, W., Cui, Y., & Song, H. (2023). Localized coupling effects and multiphysics modeling for the laser ablation behavior of composite structure subjected to high-speed airflow. *International Journal of Thermal Sciences*, *187*, 108174.

Żurawka, P., Sahbon, N., Pytlak, D., Sochacki, M., Puchalski, A., & Murpani, S. (2023, March). Multi-objective optimization of a fin shape for a passive supersonic rocket stage. In *2023 IEEE Aerospace Conference* (pp. 1-12). IEEE.

Amr Abbass
Engineering University of Idaho,
USA
Calgary732@outlook.com
ORCID: 0009-0007-9376-266X